

# Modulation Schemes for Cognitive Radio in White Spaces

Zsolt KOLLÁR, Péter HORVÁTH

Department of Broadband Infocommunications and Electromagnetic Theory, Budapest University of Technology and Economics, Goldmann Gy. tér 3., H-1111 Budapest, Hungary

kollar@mht.bme.hu, hp@mht.bme.hu

**Abstract.** *In this paper we give an overview and a comparison of the possible waveforms for white space applications. Four physical layer schemes for cognitive radio are selected for study: Orthogonal Frequency Division Multiplexing (OFDM), DFT-Spread OFDM (DFTS-OFDM), Constant Envelope OFDM (CE-OFDM) and Filter Bank Multicarrier (FBMC). The comparison is mainly based on the side effects of various non-ideal analog components (power amplifier, local oscillator) and residual synchronization errors such as frequency offset. As we will show, each technique has different sensitivity to the various impairments. The comparisons will be performed via spectral density functions and bit error rates (BER).*

## Keywords

Cognitive radio, physical layer, Orthogonal Frequency Division Multiplexing, DFT-spread OFDM, Constant Envelope OFDM, Filter Bank Multicarrier, synchronization error, white space.

## 1. Introduction

Since Mitola introduced the idea of Cognitive Radio (CR) [1] the interest has been rapidly emerging in it. The idea of CRs in white space [2], [3] is to install an opportunistic communication system in a given frequency band which remains hidden from the incumbent system. Nevertheless, it is also important that the opportunistic system should not disturb the incumbent one by any means. The opportunistic system scans the band for gaps in the spectra which could be used for transmission. The standardization of CR for white space has also been started by IEEE, currently it is in draft stage [4], [5]. These systems will be especially important with the new era of digital television which induces spectral white spaces left behind by ceased analog transmissions [2].

Naturally, there are many difficulties which have to be overcome such as spectral sensing, spectrum management and band allocation. The key question is the choice of the

applied modulation scheme. Initial studies on the safe coexistence between incumbent TV broadcast systems and potential white space devices have recommended guard channels to protect nearby incumbents. Furthermore, they called for very strict adjacent channel leakage requirements on the signal emitted by the opportunistic device. These requirements triggered intense research activities to find feasible modulation techniques that exhibit very small adjacent channel leakage [6].

Orthogonal Frequency Division Multiplexing (OFDM) [7] is often preferred in wideband wireless communication systems because extensive literature is available on it. Although OFDM has many advantages it also has some crucial drawbacks: it is highly sensitive to nonlinear distortion, synchronization errors and it exhibits moderate adjacent channel leakage. Due to these phenomena several multicarrier schemes have been proposed in the recent years which could compete with OFDM.

In this paper we selected three of the most promising alternatives for investigation: Constant Envelope OFDM [8], DFT-Spread OFDM [9], and the Filter Bank Multicarrier [10], [11] system. We investigate these schemes by means of sensitivity to nonlinear effects caused by the power amplifier. We also focus on various synchronization imperfections and their negative effects on the system performance. We will show that each modulation technique has a different sensitivity to the various effects. These parameters have to be taken into account when designing a wireless communication system for cognitive radio in white spaces.

The paper is organized as follows. In the next Section the four modulation schemes are described and the required signal processing steps are explained. Then, the transmission chain signal model is described with a detailed explanation of both the transceiver chain and the digital baseband model with impairments of the various analog elements. In the fourth Section simulation results are given for various impairments of the transmission path such as nonlinear power amplifier, residual frequency offset, phase error/jitter and IQ-mismatch. Finally, the conclusion is drawn from the results of the simulations and an overview is given for the four modulation schemes regarding the various impairments.

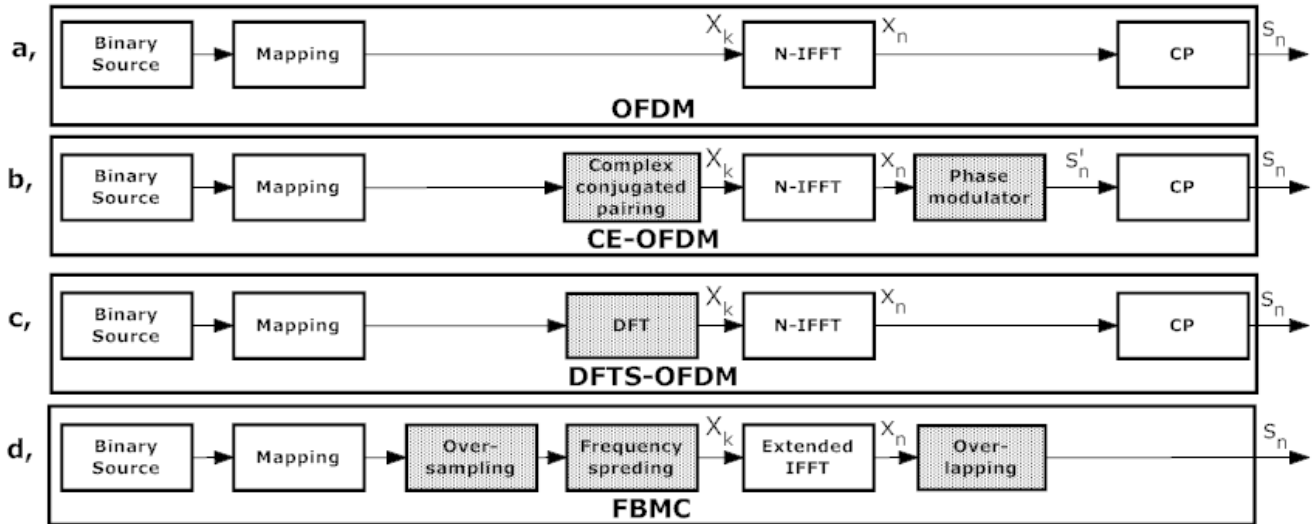


Fig. 1. Block diagram of the following modulation schemes: OFDM (a), CE-OFDM (b), DFT-OFDM (c), FMBC (d).

## 2. Transmitter Models

In this section we discuss and introduce the basic block diagrams of the investigated schemes comparing also their signal processing complexity. A general block diagram of the four studied multicarrier modulation systems can be seen in Fig. 1. All modulation schemes include a block performing Inverse Fourier Transform (IFFT). The difference lies mainly in the surrounding signal processing blocks.

### 2.1 OFDM

The block diagram of an OFDM transmitter is depicted in Fig. 1(a). The popularity of the system lies in the fact that the modulation and demodulation can be performed simply by using Inverse Fast Fourier Transform (IFFT) and Fast Fourier Transform (FFT) respectively. The time domain samples of an OFDM symbol can be calculated using an N point IFFT as

$$x_n = \sum_{k=0}^{N-1} X_k e^{j\frac{2\pi}{N}nk}, \quad n = 0, 1, \dots, N-1 \quad (1)$$

where  $X_k$  is the complex modulation data for the subcarrier with index  $k$ . Then, prior to transmission, a Cyclic Prefix (CP) is added to each symbol. With the use of the CP the inter symbol interference can be overcome, but it reduces the effective data rate of the system. On the other hand, OFDM has some well known drawbacks:

- To perform carrier interference free demodulation, the subcarriers have to remain orthogonal, otherwise the system performance will degrade. Therefore, OFDM is very sensitive to the frequency offset originating from the mismatch of transmitter and receiver local oscillators.
- The time domain OFDM signal is the sum of a large number of complex sinusoids, which means that, ac-

ording to the central limit theorem, the amplitude distribution tends to be Gaussian, leading to a large peak-to-average power ratio (PAPR) of the signal. Hence, a power amplifier with a relatively large linear range is required, otherwise nonlinear effects will severely degrade the system performance and out of band radiation will appear.

### 2.2 CE-OFDM

CE-OFDM [8] aims to solve the high PAPR values of the OFDM signal. The complex modulation symbols are aligned in a complex conjugated manner to achieve a real-valued IFFT output as depicted in Fig. 1(b). Subsequently, phase modulation is applied to the real-valued time domain signal and the CP is added to form the transmitted signal. The transmitted symbol  $s'_n$  before adding the CP can be expressed as:

$$s'_n = e^{j2\pi m x_n}, \quad n = 0, 1, \dots, N-1 \quad (2)$$

where  $m$  is the modulation index of the phase modulator and  $x_n$  is defined in (1) but with the restriction of  $X_k = X_{N-k}^*$ . A noticeable disadvantage is that the complex conjugated pairing reduces the data rate by a factor of two. Then the phase modulator can be driven by this real valued signal that results in a constant envelope output signal. The power spectrum density (PSD) of the transmitted signal will be determined by the modulation index  $m$  of the phase modulator.

### 2.3 DFTS-OFDM

In case of DFTS-OFDM systems [9], the complex modulation data set is preprocessed, the complex modulation values which will be transmitted are grouped and a DFT is applied as can be seen in Fig. 1(c). Then the output of the DFT is used to modulate the subcarriers. This technique can

be also considered as a single carrier modulation scheme, where the frequency spreading is applied through all subcarriers. The result is a slightly lower PAPR value compared to OFDM transmission.

### 2.4 FBMC

FBMC systems [10], [11] use a specially designed filter bank structure. First the complex modulation values are spread over several carriers and filtered by a prototype filter. This implies the necessity of a larger FFT to construct the transmission signal, which can be seen in Fig. 1(d). Due to the advantageous properties of the prototype filter bank, the spectral band efficiency will be more efficient than the OFDM signal. With the use of an offset-QAM modulation, where the real and imaginary data values are offset by half symbol duration, no data rate loss will occur. Prior to transmission the symbols are overlapped in such a way that they can be separated at the receiver due to the fact that the filter bank is designed to fulfill the Nyquist criterion to minimize the inter-symbol interference. Although the symbols duration is longer compared to OFDM symbols and they overlap, no data rate loss will occur. The other advantage of FBMC is that no CP has to be used to compensate the channel-induced inter-symbol interference. However, more complex signal processing has to be applied, and the channel equalization in the receiver chain will be more complex than in case of other schemes. With the use of a so called polyphase filterbank [10] the previously mentioned signal processing requirement can be reduced.

## 3. Transceiver Model

In this section the transceiver model is described in details. First the transmitter – channel – receiver chain is described from the hardware point of view, then the complex digital baseband equivalent is given with the model for each investigated analog component with their impairments.

### 3.1 Transmission Chain

A simplified model of the transceiver chain can be seen in Fig. 2.

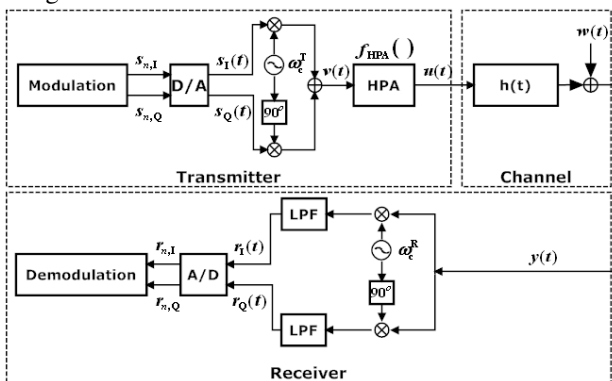


Fig. 2. Model of the transceiver chain.

After the modulation, the In-phase (I)  $s_{n,I}$  and Quadrature (Q)  $s_{n,Q}$  components of the discrete complex baseband signal  $s_n$  are converted to analog signals  $s_I(t)$  and  $s_Q(t)$  by D/A converters. The next step is the pass-band modulation which is performed by a multiplication with the cosine and sine signals generated by the transmitter local oscillator with the frequency  $\omega_c^T$  and adding them together. The pass-band signal can be expressed as:

$$v(t) = \Re\{s(t)e^{j\omega_c^T t}\} \tag{3}$$

where  $\Re\{\}$  means the real part of the argument. Next, the pass-band signal is amplified using a high power amplifier (HPA). The output signal  $u(t)$  is formed on the bases of the characteristics of the amplifier:

$$u(t) = f_{HPA}(v(t)). \tag{4}$$

The radio channel is modeled by a tap-delay line having an impulse-response of  $h(t)$  representing the multipath propagations and an additive white gaussian noise (AWGN) term  $w(t)$ . Having passed the channel, the signal  $u(t)$  form the received signal  $y(t)$  as:

$$y(t) = u(t) * h(t) + w(t). \tag{5}$$

The received signal  $y(t)$  is converted down to the baseband using the receiver LO with the frequency  $\omega_c^R$ . The signals I and Q are segmented from the downconverted signal using a low pass filter (LPF):

$$r_I(t) = \Re\{y(t)e^{-j\omega_c^R t}\}, \tag{6}$$

$$r_Q(t) = \Im\{y(t)e^{-j\omega_c^R t}\} \tag{7}$$

where  $\Re\{\}$  and  $\Im\{\}$  mean the real and the imaginary part of the argument. The baseband I and Q signals are then sampled using an A/D converter forming the signals  $r_{n,I}$  and  $r_{n,Q}$  which are passed to the digital demodulator and processed according to the modulation scheme.

### 3.2 Digital Baseband Model with Impairments

The digital baseband transmission path can be divided into three major parts as it is depicted in Fig. 3.

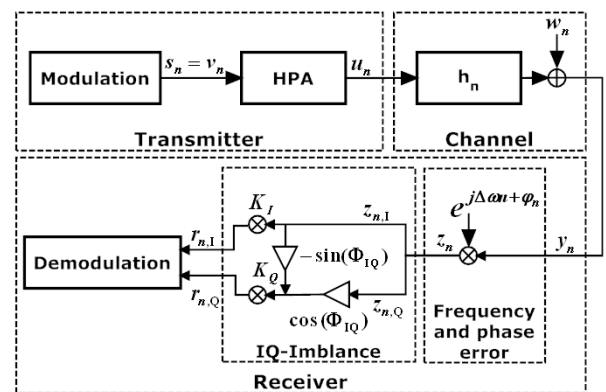


Fig. 3. Complex discrete baseband model with impairments for the transceiver chain.

Every component is considered in the complex digital baseband: the baseband equivalent of the channel is applied and the errors caused by the up- and downconversion is shifted to the receiver. In our model we only consider the error caused by the nonlinear HPA at the transmitter side. The channel consists of the channel filter and an AWGN term. Finally, three types of errors are introduced at the receiver: frequency and phase errors of the local oscillators and the IQ-mismatch. The model for each error is discussed in the following sections.

- **Amplifier**

The high power amplifier (HPA) is a crucial element of the transmitter chain. These analog components are not ideal, they have a limited linear range, which may introduce nonlinear distortions. For the baseband equivalent of the high power amplifier (HPA) a memoryless Saleh-model [12] was applied which has the following discrete amplitude transfer function  $A_{\text{HPA}}(|v_n|)$  and phase shift characteristics  $\Phi_{\text{HPA}}(|v_n|)$ :

$$A_{\text{HPA}}(|v_n|) = \frac{\alpha|v_n|}{1 + \beta|v_n|}, \quad (8)$$

$$\Phi_{\text{HPA}}(|v_n|) = \frac{\rho|v_n|}{1 + \lambda|v_n|^2} \quad (9)$$

where  $|v_n|$  is the amplitude of the input signal  $v_n$  and  $\alpha$ ,  $\beta$ ,  $\rho$ ,  $\lambda$  are the parameters of the HPA. The output signal  $u_n$  can be expressed

$$u_n = A_{\text{HPA}}(|v_n|)e^{j(\angle(v_n) + \Phi_{\text{HPA}}(|v_n|))} \quad (10)$$

where  $\angle(v_n)$  is the phase of the complex baseband signal  $v_n$ .

- **Channel**

For the channel, the digital baseband equivalent is used. It means that the output of the channel can be expressed as the discrete convolution of the input signal and the channel impulse response, and an added AWGN sample:

$$y_n = u_n * h_n + w_n. \quad (11)$$

- **Frequency and Phase Errors**

Frequency and phase error occurs during up and down conversion of the baseband signal to the passband. A detailed description is given in [15]. Frequency error  $\Delta\omega$  is the result of local oscillator (LO) mismatches between the transmitter and receiver side:

$$\Delta\omega = \omega_c^T - \omega_c^R. \quad (12)$$

The frequency offset is measured in terms of carrier spacing. Usually, the frequency errors are estimated based on known preambles so in our simulation we will only consider small residual frequency errors. We do not consider the effect of the phase shift caused by the frequency offset. The phase errors  $\varphi_n$  are caused by the phase jitter of the local oscillators and the phase

mismatch between them. The constant phase shift can be estimated via channel estimation and corrected at the channel equalization. So we attempt to focus on the phase jitter which can be modeled as a variable  $\varphi \sim N(0, \sigma_\varphi^2)$  having a normal distribution. The resulting signal  $z_n$  can be written as

$$z_n = y_n e^{j\Delta\omega n + \varphi_n}. \quad (13)$$

- **IQ-mismatch**

IQ-mismatch is also an adverse consequence of down conversion. The error is generated when an amplitude imbalance or a quadrature error (phase difference is not exactly  $90^\circ$ ) occurs between the I and Q branches. The IQ-mismatch causes in general an interference between the I and Q branch. The IQ-mismatch can be simply modeled according to [14] by two parameters: The amplitude imbalance  $K$  and the quadrature error  $\phi_{\text{IQ}}$ . The value  $K$  represents the power mismatch between the I and Q branches, which is represented by the constants  $K_I$  and  $K_Q$ . So the model can be written as

$$\begin{bmatrix} r_{n,I} \\ r_{n,Q} \end{bmatrix} = \begin{bmatrix} K_I & 0 \\ -K_Q \sin \phi_{\text{IQ}} & K_Q \cos \phi_{\text{IQ}} \end{bmatrix} \begin{bmatrix} z_{n,I} \\ z_{n,Q} \end{bmatrix}. \quad (14)$$

## 4. Simulation Results

In this section the system parameters used for the simulation are given, then the effect of each imperfection on the system performance is analyzed separately. The system performances are compared via the bit error rate as a function of signal to noise ratio (SNR). In our case the SNR values are defined as

$$\text{SNR}_{\text{dB}} = 10 \log_{10} \left( \frac{E_s}{N_0} \right) \quad (15)$$

$$= 10 \log_{10} \left( \frac{E_b N_c M}{OV(N+CP)N_0} \right) \quad (16)$$

with  $E_b$  being the bit energy,  $N_0$  the noise variance.  $N$  is the number of the subcarriers available and  $N_c$  is the number of subcarriers used.  $CP$  is the length of the cyclic prefix in samples,  $OV$  is the oversampling ratio and  $M$  is the number of bits transmitted by one subcarrier. For the simulations we applied a 64-FFT with a cyclic prefix of 16 samples and an oversampling ratio of 4. We applied 16-QAM on 48 subcarriers from the maximally available 64, leaving out the DC subcarrier and some carriers on the edge of the transmission band. For the DFTS-OFDM we used a 48 point DFT for pre-processing. For the CE-OFDM modulation we have chosen a moderate modulation index of  $h = 0.8$ . The bit error rates are compared to the above mentioned simulation parameters, plotting the values in the function of the normalized  $\frac{E_b}{N_0}$ . The results of the simulations are shown in Fig. 4.

In the absence of nonlinear distortions and synchronization errors the FBMC outperforms all the other modulations, due to the fact that it has no CP added to the transmitted signal, resulting the best data rate. The worst bit error

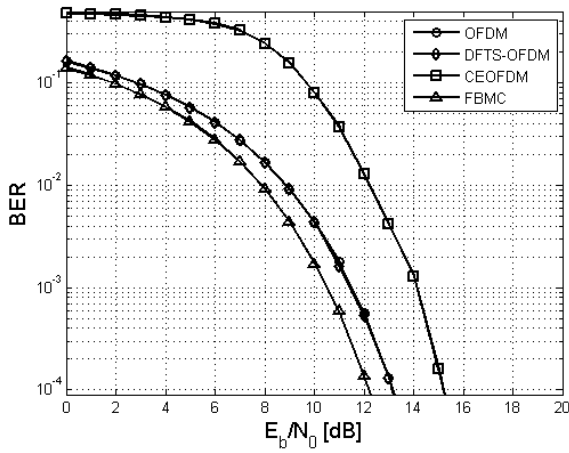


Fig. 4. Bit error rate of the four schemes over AWGN channel.

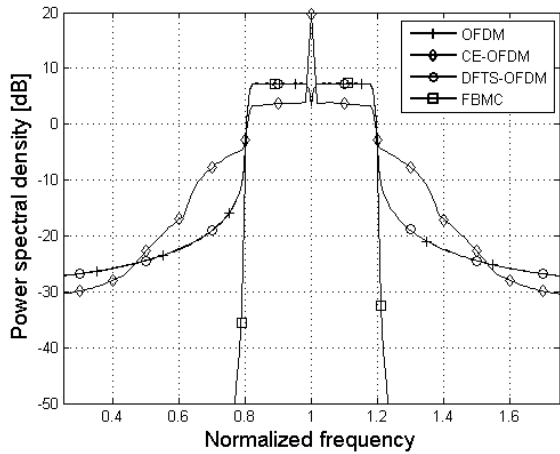


Fig. 5. Power spectrum density function for the four modulation schemes.

rate can be observed with CE-OFDM modulation, due to the fact that it incurs a data rate loss of  $\frac{1}{2}$  which is significantly smaller in comparison with the others.

Another important measure of the transmitted signal is its spectral behavior especially regarding the out-of-channel leakage. These measures are especially important when dealing with white space scenarios. The power spectrum density functions of the transmitted signal with a linear HPA can be seen in Fig. 5. It can be observed that FBMC outperforms all other multicarrier schemes.

### 4.1 Amplifier Nonlinearity

First we have investigated the negative effects of the nonlinear HPA. In the simulation scenario we used parameters similar to [13] but with slightly smoother nonlinearity:  $\alpha = 1$ ,  $\beta = 0.05$ ,  $\rho = \frac{\pi}{32}$ ,  $\lambda = 0.125$ . The bit error rate results are depicted in Fig. 6.

It can be observed that CE-OFDM is very robust against the effects of the HPA, due to its constant envelope.

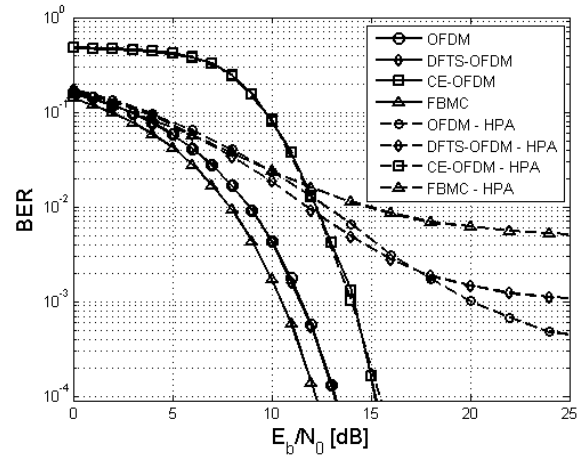


Fig. 6. Bit error rate of the four schemes over AWGN channel with the effect of a nonlinear HPA ( $\alpha = 1$ ,  $\beta = 0.05$ ,  $\rho = \frac{\pi}{32}$ ,  $\lambda = 0.125$ ).

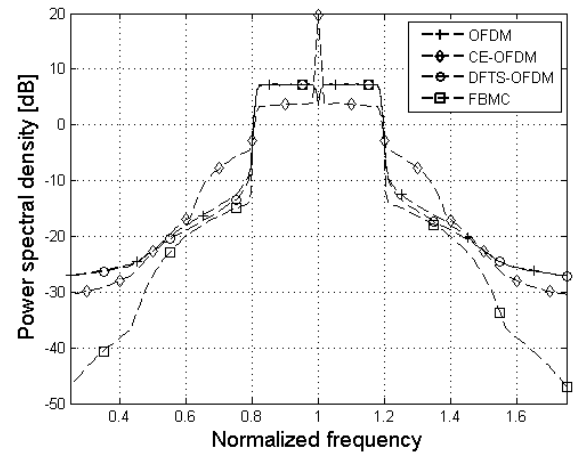


Fig. 7. Power spectrum density function for the four modulation schemes with nonlinear power amplifier.

On the other hand, the performance of FBMC is severely degraded. A slightly better performance can be observed at the SC-FDMA system which is also outperformed after about 17 dB by OFDM. It can be concluded that with the exception of CE-OFDM, all other modulations are very sensitive to nonlinear distortions.

An equally important measure is the occupied bandwidth, which can be compared via power spectrum density functions. The distorted spectra are depicted in Fig. 7. If we compare it with the ideal case shown in Fig. 5 we can see that the power spectrum density function of FBMC is highly distorted, although the out-of-band emission is still smaller than that of the other three schemes.

### 4.2 Frequency Mismatch

For the LO mismatch we choose a relatively small residual frequency difference of  $\Delta\omega = 0.03$  subcarrier spacing. The resulting bit error rate curves are depicted in Fig. 8. It can be seen that in this case CE-OFDM is the most

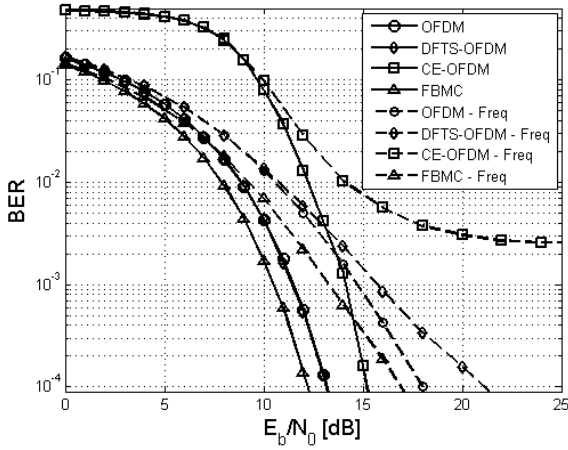


Fig. 8. Bit error rate of the four schemes over AWGN channel with the effect LO mismatch  $\Delta\omega = 0.03$  subcarrier spacing.

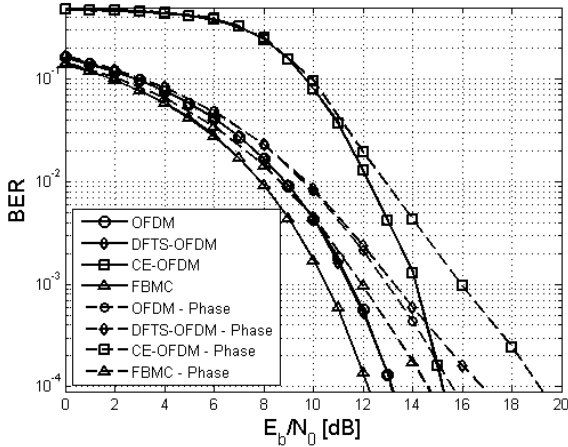


Fig. 9. Bit error rate of the four schemes over AWGN channel with the effect of a phase jitter ( $\varphi \sim N(0, \sigma_\varphi = 8^\circ)$ ).

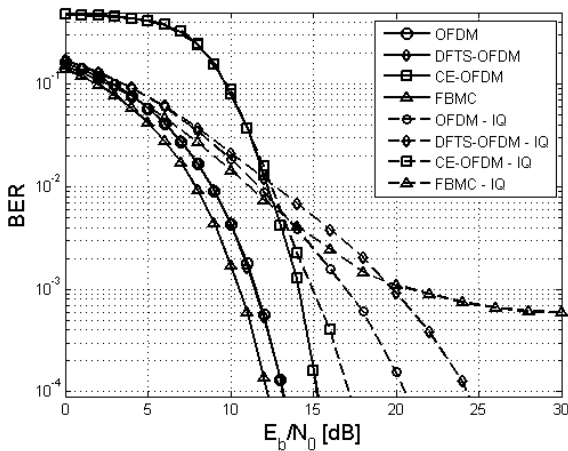


Fig. 10. Bit error rate of the four schemes over AWGN channel with the effect of IQ-mismatch:  $K = 0.87$  dB,  $K_I = 0.95$ ,  $K_Q = 1.05$ ,  $\phi_{IQ} = 10^\circ$ .

sensitive, it hits a bit error floor of  $2 \cdot 10^{-3}$  above 20 dB. Regarding the other schemes, the FBMC still performs best, OFDM is about 1 dB and DFTS-OFDM is about 5 dB worse in performance.

### 4.3 Phase Noise

The system performance in the presence of a normally distributed ( $\varphi \sim N(0, \sigma_\varphi = 8^\circ)$ ) phase jitter can be seen in Fig. 9. As it can be suspected the performance of CE-OFDM is affected most severely by the phase jitter. The performance degradation of FBMC, OFDM, DFTS-OFDM is similar to the case of the frequency mismatch of the LOs.

### 4.4 IQ-Mismatch

The results for IQ-mismatch are plotted in Fig. 10. The applied parameters were:  $K = 0.87$  dB,  $K_I = 0.95$ ,  $K_Q = 1.05$ ,  $\phi_{IQ} = 10^\circ$ . CE-OFDM has the largest immunity to IQ-mismatch. The performance of OFDM is about 3 dB and the performance of DFTS-OFDM is about 6 dB worse. FBMC modulation reaches a bit error floor of  $5 \cdot 10^{-4}$ , but its performance is better than DFTS-OFDM below 19 dB.

## 5. Conclusion

In this paper we introduced four possible choices for the modulation scheme for cognitive radios in white space. A model was given for the complex discrete baseband transceiver chain including the transmission channel. We have compared these schemes by means of the effects of various imperfections in the transfer chain, namely: HPA nonlinearity, frequency offset, phase jitter and IQ-mismatch. The influence of these errors on the bit error rate was examined and it has been shown that each modulation type has its own strength and weakness depending on the type of introduced imperfectness. An overview of the results is given in Tab. 1. Black color means that the given scheme performs the worst in the presence of a given error. White color means that it has the best performance and gray shading means that its performance is not the best, but it is just a few dBs worse in comparison with the best.

Modulation name	HPA	$\Delta\omega$	$\varphi$	$IQ$
OFDM				
CE-OFDM				
DFTS-OFDM				
FBMC				

Tab. 1. Comparison of the four modulation schemes. Best performance depicted in white, the worst is given with black color, intermediate performance is with gray color.

## Acknowledgements

The research leading to these results was derived from the European Community's Seventh Framework Programme (FP7) under Grant Agreement number 248454 (QoSAMOS).

## References

- [1] MITOLA, J., MAGUIREM, G. Q. Cognitive radio: Making software radios more personal. *IEEE Personal Communications*, 1999, vol. 6, no. 4, p. 13 – 18.
- [2] SHELLHAMMER, S. J., SADEK, A. K., WENYI ZHANG. Technical challenges for cognitive radio in the TV white space spectrum. In *Information Theory and Applications Workshop*. San Diego (USA), 2009, p. 323 – 333.
- [3] BORTH, D., EKL, R., OBERLIES, B., OVERBY, S. Considerations for successful cognitive radio systems in US TV white space, *3rd IEEE Symposium on Dynamic Spectrum Access Networks DySPAN 2008*. Chicago (USA), 2008, p. 1 – 5.
- [4] IEEE 802.22 Working Group on Wireless Regional Area Networks. [Online]. Available at: <http://www.ieee802.org/22/>
- [5] CORDEIRO, C., CHALLAPALI, K., BIRRU, D., SHANKAR, S. IEEE 802.22: The first worldwide wireless standard based on cognitive radios. In *IEEE International Symposium on Dynamic Spectrum Access Networks DySPAN*. Baltimore (USA), 2005, p. 328 – 337.
- [6] Federal Communications Commission. *Second Memorandum Opinion and Order: In the Matter of Unlicensed Operation in the TV Broadcast Band and Additional Spectrum for Unlicensed Devices Below 900 MHz in the 3 GHz Band*. [Online]. 2010. Available at: [http://www.fcc.gov/Daily\\_Releases/Daily\\_Business/2010/db0924/FCC-10-174A1.pdf](http://www.fcc.gov/Daily_Releases/Daily_Business/2010/db0924/FCC-10-174A1.pdf).
- [7] VAN NEE, R., PRASAD R. *OFDM for Wireless Multimedia Communications*. Boston (USA): Artech House, 2000.
- [8] THOMPSON, S. C., AHMED, A. U., PROAKIS, J. G., ZEIDLER, J. R., GEILE M. J. Constant-envelope OFDM. *IEEE Transactions on Communication*, 2008, vol. 56, no. 8., p. 1300 – 1312.
- [9] HYUNG, G. M., JUNSUNG, L., GOODMAN, D. J. Single carrier FDMA for uplink wireless transmission. *IEEE Vehicular Technology Magazine*, 2006, vol. 1, no. 3, p. 30 – 38.
- [10] VAIDYANATHAN, P. P. *Multirate Systems and Filter Banks*. Upper Saddle River (USA): Prentice-Hall, 1993.
- [11] PAYARÓ, M., PASCUAL-ISERTE, A., NÁJAR, M. Performance comparison between FBMC and OFDM in MIMO systems under channel uncertainty. In *Proc. IEEE European Wireless EW 2010*. Lucca (Italy), 2010.
- [12] SALEH, A. Frequency-independent and frequency-dependent non-linear models of TWT amplifiers. *IEEE Transactions on Communication*, 1981, vol. 29, p. 1715 – 1720.
- [13] ALI, S., MARKARIAN, G., AL-AKAIDI, M. Frequency domain iterative compensation of high power amplifier non-linearity. In *Middle Eastern Multiconference on Simulation and Modelling MESM 2008*. Amman (Jordan), 2008.
- [14] HELD, I., KLEIN, O., CHEN, A., MA, V. Low complexity digital IQ imbalance correction in OFDM WLAN receivers. In *Vehicular Technology Conference VTC 2004-Spring*. Milan (Italy), 2004, vol. 2, p. 1172 – 1176.
- [15] POLLET, T., VAN BLADEL, M., MOENECLAHEY, M. BER sensitivity of OFDM systems to carrier frequency offset and wiener phase noise. *IEEE Transactions on Communication*, 1995, vol. 43, p. 191 – 193.

## About Authors ...

**Zsolt KOLLÁR** was born in Budapest, Hungary, in 1983. He received his M.Sc. degree in electric engineering from the Budapest University of Technology and Economics in 2008. He is currently working towards his Ph.D degree. He joined the Rohde&Schwarz reference laboratory in 2007, where he is currently a development engineer. His research interests include digital signal processing, channel coding and wireless communication.

**Péter HORVÁTH** was born in Budapest, Hungary, in 1978. He is currently an assistant lecturer at the Budapest University of Technology and Economics. His research interests include MIMO communications, channel modeling and physical layer aspects of cognitive radio.